http://doi.org/10.35784/iapgos.7570 *received: 14.04.2025 | revised: 31.10.2025 | accepted: 18.11.2025 | available online: 20.12.2025*

MODELLING OF DYNAMIC PROCESSES IN A NONHOLONOMIC SYSTEM IN THE FORM OF GIBBS-APPELL EQUATIONS ON THE EXAMPLE OF A BALL MILL

Volodymyr Shatokhin[1], Yaroslav Ivanchuk[2], Vitaly Liman[3], Sergii Komar[4], Oleksii Kozlovskyi[2]
[1]O. M. Beketov National University of Urban Economy in Kharkiv, Department of Theoretical and Applied Mechanics, Kharkiv, Ukraine, [2]Vinnytsia National Agrarian University, Department of Computer Science, Vinnytsia, Ukraine, [3]Vinnytsia National Agrarian University, Department of Computer Science and Economic Cybernetics, Vinnytsia, Ukraine, [4]Ivan Kozhedub Kharkiv National University of the Air Force, Department of Aeronautical Engineering, Kharkiv, Ukraine

Abstract. *In the article the actual scientific and practical problem of creation of the universal mathematical model of dynamic processes in the shockless model of the ball mill is solved. This allowed to determine the technological qualities of the device and to make an effective choice of its rational parameters. Computational studies have been carried out using the developed model by means of computer calculations. As a result, important regularities of the influence of parameters on the technological indicators of the technological device have been established. The result of the study is the first development of a nonholonomic mathematical model of dynamic processes in a ball mill, presented in the form of Gibbs-Appell equations. It is shown that the calculation of the acceleration energy and the formulation of the equations of motion are significantly simplified when quasi-accelerations are used instead of generalised acceleration equations. The developed mathematical model allows to calculate the trajectories of the contact point of the ball with the surface of the spherical chamber, the compressive forces of interaction with the surface of the shell. The results of the mathematical modelling allow efficient selection of rational parameters of the process equipment from the technological point of view.*

Keywords: ball milling, dynamic system, mathematical model, differential equations, velocity, acceleration

MODELOWANIE PROCESÓW DYNAMICZNYCH W UKŁADZIE NIEHOLONOMICZNYM W POSTACI RÓWNANIA GIBBSA-APPELLA NA PRZYKŁADZIE MŁYNA KULOWEGO

Streszczenie. *W artykule rozwiązano aktualny problem naukowy i praktyczny dotyczący stworzenia uniwersalnego modelu matematycznego procesów dynamicznych w bezuderzeniowym modelu młyna kulowego. Pozwoliło to określić właściwości technologiczne urządzenia i dokonać skutecznego wyboru jego racjonalnych parametrów. Przeprowadzono badania obliczeniowe z wykorzystaniem opracowanego modelu za pomocą obliczeń komputerowych. W rezultacie ustalono istotne prawidłowości wpływu parametrów na wskaźniki technologiczne urządzenia technologicznego. Wynikiem badań jest pierwsze opracowanie nieholonomicznego modelu matematycznego procesów dynamicznych w młynie kulowym, przedstawionego w postaci równań Gibbsa-Appella. Wykazano, że obliczenia energii przyspieszenia i sformułowanie równań ruchu są znacznie uproszczone, gdy zamiast uogólnionych równań przyspieszenia stosuje się quasi-przyspieszenia. Opracowany model matematyczny pozwala obliczyć trajektorie punktu styku kulki z powierzchnią komory sferycznej oraz siły ściskające oddziaływania z powierzchnią powłoki. Wyniki modelowania matematycznego pozwalają na efektywny dobór racjonalnych parametrów urządzeń procesowych z technologicznego punktu widzenia.*

Słowa kluczowe: mielenie kulowe, układ dynamiczny, model matematyczny, równania różniczkowe, prędkość, przyspieszenie

Introduction

Crushing and grinding of various materials are crucial in many technological processes. In modern production of finely dispersed products, drum mills – in which the grinding elements are balls – are widely used [3]. The main advantages of ball mills include their simple design, ease of operation and maintenance, high reliability, large unit capacity, flexibility in adjusting grinding modes to obtain a homogeneous product, ability to achieve fine grinding with a high specific surface area, and a well-established theoretical foundation [1, 16].

However, ball mills also have certain disadvantages, such as high metal consumption and wear of the grinding media, significant noise (especially in impact – cascade mode), and the presence of stagnant zones [4]. Most of the energy consumed during the operation of a ball mill is dissipated, resulting in low efficiency [19]. Nevertheless, even considerable specific energy consumption is often justified by the advantages of using such mills. This, however, does not eliminate the need to search for energy-saving solutions in grinding processes, which remains an active research area for specialists worldwide [6, 15].

The purpose of this study is to develop a universal mathematical model of the dynamic processes occurring in a non-impact ball mill, in order to determine its technological characteristics and select its optimal parameters. The model should incorporate the main geometric and mass characteristics of the ball and the spherical chamber and account for the nonholonomic nature of the constraints imposed on the ball.

To achieve this objective, the following tasks were formulated:

- to analyse the features of technical systems whose main structural element is a ball moving within a spherical cavity;
- to develop a mathematical model of the dynamic processes in a ball mill in the form of equations of motion for a ball inside a spherical shell undergoing circular translational motion;
- to derive the differential equations of the ball's motion in the form of Gibbs-Appell equations, using the corresponding generalised coordinates and quasi-velocities, as well as holonomic (geometric) and nonholonomic constraints.

The development of methods for the rational selection of device parameters is therefore an important and timely task.

1. Analysis of latest researches and publications

Current research efforts are focused on addressing specific challenges related to the improvement of existing ball mill designs. A considerable number of publications contain information on these devices, and several papers are devoted to tackling complex problems associated with modelling their dynamic processes.

In recent years, significant progress has been achieved in understanding the key features of ball mill mechanisms, largely owing to the widespread adoption of the Discrete Element Method (DEM), which has become an essential tool for modelling dynamic processes in ball mills. Studies of dry-operating mills – encompassing both grinding media and particles – conducted using DEM simulations have provided the foundation for several enhanced ball mill models [15].

However, modelling grinding processes using DEM remains a highly challenging task. Major difficulties arise in determining the model parameters that define the interactions between particles, balls, and the mill lining. Moreover, values of the dynamic and static friction coefficients and restitution parameters are required for each pair of materials involved in the grinding process. The problem is compounded by the absence of well-established methods for determining these parameters, which necessitates dedicated experimental studies to investigate the influence of various factors on the grinding

process. It should be noted, however, that the development of an adequate model enables researchers to dispense with costly real-world experiments, which are often difficult to perform in practice [6].

The authors of O. Manzhilevskyy [10] and X. Zhang [20] proposed a new model of ball mill in which the working chamber is made in the form of a spherical shell. The working body of the mill is a ball inside the chamber, which, when the shell moves, rolls its inner surface, destroying and grinding cement or other raw materials. This design eliminates shock modes during operation and does not create stagnant zones.

In recent years, similar design schemes have been used in ball vibration absorbers [13] as an alternative to passive vibration absorbers [18]. The latter are often used in civil engineering to reduce wind-induced vibrations. Conventional pendulum-type passive absorbers use autoparametric resonance to provide damping. Although they are very effective and reliable, their use is often hampered by a lack of installation space or maintenance complexity.

The paper of M. Pirner [14] describes the theory, experiments and practical application of a ball vibration absorber with horizontal displacement and its effectiveness in comparison with a pendulum vibration absorber. The system is considered to be non-holonomic. It includes two solids that perform a plane motion: a column and a ball that rolls without slipping along a spherical cavity.

In article of J. Náprstek [11] Lagrange's equations of the second kind are used to model the dynamic processes in a ball vibration absorber. The second Lyapunov method is used as the main tool to study the dynamic stability.

A similar problem related to the antiseismic protection of buildings has been considered, for example, in V. Legeza [7]. A nonholonomic dynamic model is constructed using the Gibbs-Appell method. In this case, the problem formulation is simplified and nonholonomic constraint functions are introduced easily and clearly.

The paper of J. Náprstek [12] investigates the response of a heavy ball rolling in a hemispherical cavity under horizontal kinematic excitation. A system with six degrees of freedom and three nonlinear binders is considered. The contact between the ball and the cavity surface is assumed to be perfect, without slippage. The mathematical model is constructed using the Gibbs-Appell acceleration energy function. Numerical experiments are carried out with different excitations at a slow change of frequency. Examples of the use of this scheme as a vibration absorber in some building structures are described. A comparison with a conventional pendulum damper is made.

The paper of [5] is devoted to the study of forced vibrations in a vibration isolation system under the action of an external harmonic load. The device consists of a ball vibration absorber with linear viscous resistance and a moving bearing body. Based on Gibbs-Appell formalism, the equations of the joint motion of a heavy ball without slipping in a spherical cavity of a bearing body are formulated and solved numerically.

For a non-holonomic dynamic model of a ball vibration absorber, the amplitude-frequency response of the system, the dependence of the maximum amplitude of the vibration of the bearing body on the radius of the spherical shell and the coefficient of resistance viscosity were constructed in article [8]. The conditions and limits of rolling of a heavy ball in a spherical cavity without slipping are determined.

It should be noted that important technical objects in which ball vibration dampers have been used recently are wind turbines. In paper of [17], a study was carried out on their use to minimise excessive vibrations and extend the fatigue life of these devices.

The fundamentals and theoretical justification of the Gibbs-Appell approach can be found in monographs such as [9] or [2, 5].

2. Materials and methods

The design of a ball mill [10, 20] is shown in Figure 1. The bearing frame is supported by two fixed supports and has its own independent drive for rotation around its own axis; a four-jointed parallelogram is installed on the frame, two sides of which are cranks; the cranks have an independent drive and rotate synchronously; a platform is fixed at the ends of the cranks as one of the sides of the parallelogram; the platform makes a circular translational movement; a spherical shell is installed on the platform, inside which there is a ball which is the working body of the mill; the ball, when the shell moves, rolls around its inner surface, destroying and abrading the corresponding raw material.

The following notations have been adopted: 1 – fixed support; 2 – shaft; 3, 6 – gear; 4 – driving gear; 5 – relative rotation drive; 7 – frame (shaft); 8 – rotation drive; 9, 15 – crank; 10 – platform; 11 – cover; 12 – ball; 13 – shell; 14 – material (clinker). The proposed scheme eliminates the impact and dead zone.

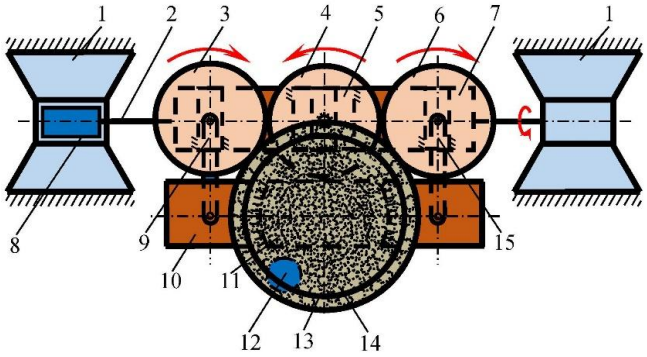

Fig. 1. Schematic diagram of a ball mill

This paper examines the motion of a ball, as the main working body of a mill, when a spherical chamber is moved, given the law of rotation of the cranks.

Let us consider the motion of a ball in a spherical chamber with centre at point *A* and radius *R*, which has a given translational motion (Fig. 2). In this case, the chamber can be considered as an unsteady linkage. The radius of the ball centred at point *C* is denoted by *r* and the point of its contact with the spherical surface is denoted by *P*. Let us introduce the basic (fixed) coordinate system $O_1x_1y_1z_1$ and the moving coordinate system *Oxyz*, which moves translationally.

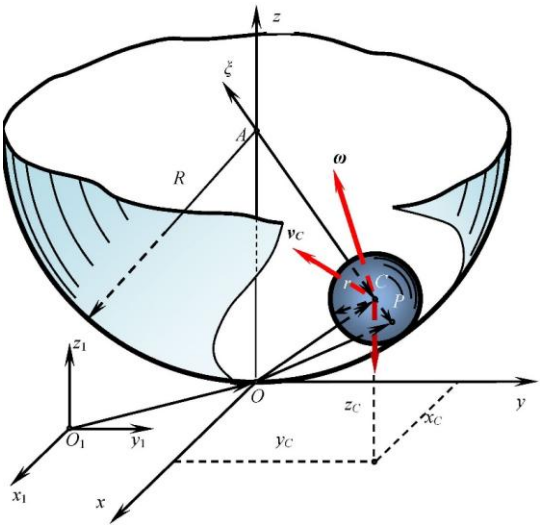

Fig. 2. Design scheme of ball movement in a spherical mill chamber

For the independent generalised coordinates we take: $q_1 = x_C$, $q_2 = y_C$, $q_3 = \Psi$, $q_4 = \varphi$, $q_5 = \vartheta$, where x_C, y_C are the coordinates of the centre of mass of the sphere in the coordinate system connected to the camera; Ψ, φ, ϑ are the Euler angles that determine the position of the axes of the coordinate system rigidly connected to the sphere relative to its own coordinate axes parallel to *Ox*, *Oy*, *Oz*.

The equation of the holonomic (geometric) viscosity is expressed by equation:

$$z_C = R - \sqrt{(R-r)^2 - x_C^2 - y_C^2} \tag{1}$$

The equations of nonholonomic viscosity are obtained from the condition of no sliding of the ball on a spherical surface, which is expressed by the equality of the absolute velocities of the points of contact between the ball and the chamber:

$$\mathbf{v}_{Pa} = \mathbf{v}_{Pe} + \mathbf{v}_{Pr} = \mathbf{v}_{Oa} + \mathbf{v}_C + \boldsymbol{\omega} \times \overrightarrow{CP} = \mathbf{v}_{Oa} \tag{2}$$

where $\boldsymbol{V}_{Pa}$, $\boldsymbol{V}_{Pe} = \boldsymbol{V}_{Oa}$, $\boldsymbol{V}_{Pr}$ – the absolute, translational and relative velocities of point *P* (the translational velocity $\boldsymbol{V}_{Pe}$ in this case coincides with the absolute velocity $\boldsymbol{V}_{Oa}$ of point *O*); $\mathbf{v}_C = \mathbf{v}_{Cr} = \begin{bmatrix} \dot{x}_C & \dot{y}_C & \dot{z}_C \end{bmatrix}^{\mathrm{T}}$ – is the velocity of point *C* in the moving coordinate system (relative velocity; *T* is the transpose sign); $\boldsymbol{\omega} = \begin{bmatrix} \omega_x & \omega_y & \omega_z \end{bmatrix}^{\mathrm{T}}$ – instantaneous angular velocity of the ball.

For the $\overrightarrow{CP}$ vector, there is an obvious correlation:

$$\overrightarrow{CP} = \frac{r}{R-r}\left(\overrightarrow{OC} - \overrightarrow{OA}\right) = \lambda \begin{bmatrix} x_C \\ y_C \\ z_C - R \end{bmatrix}$$

where $\lambda = \dfrac{r}{R-r}$.

It follows from formula (2) that the relative velocity of point *P* is zero:

$$\mathbf{v}_{Pr} = \mathbf{v}_C + \boldsymbol{\omega} \times \overrightarrow{CP} = 0 \tag{3}$$

Since, based on formula (1), the projection of the velocity *C* of a point on the *z*-axis

$$\dot{z}_C = \frac{x_C \dot{x}_C + y_C \dot{y}_C}{R - z_C} \tag{4}$$

then expression (3) for $\boldsymbol{V}_{Pr}$ in expanded form is written as follows:

$$\begin{bmatrix} \dot{x}_C \\ \dot{y}_C \\ \dfrac{x_C \dot{x}_C + y_C \dot{y}_C}{R - z_C} \end{bmatrix} + \lambda \begin{vmatrix} \mathbf{i} & \mathbf{j} & \mathbf{k} \\ \omega_x & \omega_y & \omega_z \\ x_C & y_C & z_C - R \end{vmatrix} =$$

$$= \begin{bmatrix} \dot{x}_C - \lambda\left[\omega_y (R - z_C) + \omega_z y_C\right] \\ \dot{y}_C + \lambda\left[\omega_x (R - z_C) + \omega_z x_C\right] \\ \dfrac{x_C \dot{x}_C + y_C \dot{y}_C}{R - z_C} + \lambda(\omega_x y_C - \omega_y x_C) \end{bmatrix} = 0 \tag{5}$$

It is easy to show that the third element of the vector in the last column of formula (5) $\dfrac{x_C \dot{x}_C + y_C \dot{y}_C}{R - z_C} + \lambda(\omega_x y_C - \omega_y x_C)$ is a linear combination of the expressions for the first two elements. Therefore, the conditions imposed by a non-holonomic ligament are as follows:

$$\begin{cases} \dot{x}_C = \lambda\left[\omega_y (R - z_C) + \omega_z y_C\right] \\ \dot{y}_C = -\lambda\left[\omega_x (R - z_C) + \omega_z x_C\right] \end{cases} \tag{6}$$

The calculation of the acceleration energy and the formulation of the Gibbs-Appell equations is greatly simplified by using quasi-accelerations instead of generalised accelerations.

Therefore, we take the projections of the angular velocity on the *x*, *y*, *z* axes as independent quasi velocities [2, 9]:

$$\begin{cases} \dot{\pi}_1 = \omega_x = \dot{\phi}\sin\vartheta\sin\psi + \dot{\vartheta}\cos\psi \\ \dot{\pi}_2 = \omega_y = -\dot{\phi}\sin\vartheta\cos\psi + \dot{\vartheta}\sin\psi \\ \dot{\pi}_3 = \omega_z = \dot{\phi}\cos\vartheta + \dot{\psi} \end{cases} \tag{7}$$

These quasi-speeds correspond to quasi-coordinates $\pi_1 = \varphi_x$, $\pi_2 = \varphi_y$, $\pi_3 = \varphi_z$.

Thus, the configuration of the system under study (the moving ball) is determined by five generalised coordinates x_C, y_C, Ψ, φ, ϑ, but the system has only three degrees of freedom due to the two equations (6).

Let's write the equation of motion of a ball in Gibbs-Appell form [2, 9]:

$$\frac{\partial S}{\partial \ddot{\pi}_1} = \Pi_1, \ \frac{\partial S}{\partial \ddot{\pi}_2} = \Pi_2, \ \frac{\partial S}{\partial \ddot{\pi}_3} = \Pi_3 \tag{8}$$

where *S* is the Gibbs-Appell acceleration function, which in this case has the form

$$S = \frac{1}{2}\left[m\left(\ddot{x}_{1C}^2 + \ddot{y}_{1C}^2 + \ddot{z}_{1C}^2\right) + I\left(\dot{\omega}_x^2 + \dot{\omega}_y^2 + \dot{\omega}_z^2\right)\right] =$$

$$= \frac{1}{2}\left[m\left(\ddot{x}_{1C}^2 + \ddot{y}_{1C}^2 + \ddot{z}_{1C}^2\right) + I\left(\ddot{\pi}_1^2 + \ddot{\pi}_2^2 + \ddot{\pi}_3^2\right)\right] \tag{9}$$

where *m* – ball weight; $I = \dfrac{2}{5}mr^2$ – axial moment of inertia of the ball; Π_1, Π_2, Π_3 – generalised forces corresponding to quasi-coordinates π_1, π_2, π_3.

To determine the generalised forces Π_1, Π_2, Π_3 we calculate the virtual work:

$$\delta A = \Pi_1 \delta\pi_1 + \Pi_2 \delta\pi_2 + \Pi_3 \delta\pi_3 = F_x \delta x_{1C} + F_y \delta y_{1C} + F_z \delta z_{1C}$$

In this case $F_x = F_y = 0$, $F_z = -mg$. Coordinates of point *C* in a fixed coordinate system:

$$x_{1C} = x_{1O} + x_C, \ y_{1C} = y_{1O} + y_C,$$

$$z_{1C} = z_{1O} + z_C = z_{1O} + R - \sqrt{(R-r)^2 - x_C^2 - y_C^2}$$

whereby $z_{1O} = const = 0$. Then, taking into account (4) and (6):

$$\dot{z}_{1C} = \dot{z}_C = \frac{x_C \dot{x}_C + y_C \dot{y}_C}{R - z_C} = -\lambda\dot{\pi}_1 y_C + \lambda\dot{\pi}_2 x_C$$

and therefore, $\delta z_{1C} = -\lambda y_C \delta\pi_1 + \lambda x_C \delta\pi_2$.

Thus

$\delta A = -mg\left(-\lambda y_C \delta\pi_1 + \lambda x_C \delta\pi_2\right) = mg\lambda y_C \delta\pi_1 - mg\lambda x_C \delta\pi_2$, which means $\Pi_1 = mg\lambda y_C$, $\Pi_2 = -mg\lambda x_C$, $\Pi_3 = 0$.

For the projections of the acceleration of point *C*, taking into account formulas (4) and (6), we have:

$$\begin{cases} \ddot{x}_{1C} = \ddot{x}_{1O} + \ddot{x}_C = \ddot{x}_{1O} + \lambda\left[\ddot{\pi}_2 (R - z_C) - \dot{\pi}_2 \dot{z}_C + \ddot{\pi}_3 y_C + \dot{\pi}_3 \dot{y}_C\right] \\ \ddot{y}_{1C} = \ddot{y}_{1O} + \ddot{y}_C = \ddot{y}_{1O} - \lambda\left[\ddot{\pi}_1 (R - z_C) - \dot{\pi}_1 \dot{z}_C + \ddot{\pi}_3 x_C + \dot{\pi}_3 \dot{x}_C\right] \\ \ddot{z}_{1C} = \ddot{z}_C = -\lambda\ddot{\pi}_1 y_C + \lambda\ddot{\pi}_2 x_C - \lambda\dot{\pi}_1 \dot{y}_C + \lambda\dot{\pi}_2 \dot{x}_C. \end{cases}$$

When writing these formulas, it is taken into account that $\ddot{z}_{1O} = 0$.

Let's rewrite the formulas in another form:

$$\begin{cases} \ddot{x}_{1C} = \lambda(R - z_C)\ddot{\pi}_2 + \lambda y_C \ddot{\pi}_3 + \lambda(\dot{\pi}_3 \dot{y}_C - \dot{\pi}_2 \dot{z}_C) + \ddot{x}_{1O} \\ \ddot{y}_{1C} = -\lambda(R - z_C)\ddot{\pi}_1 - \lambda x_C \ddot{\pi}_3 - \lambda(\dot{\pi}_3 \dot{x}_C - \dot{\pi}_1 \dot{z}_C) + \ddot{y}_{1O} \\ \ddot{z}_{1C} = -\lambda y_C \ddot{\pi}_1 + \lambda x_C \ddot{\pi}_2 - \lambda(\dot{\pi}_1 \dot{y}_C - \dot{\pi}_2 \dot{x}_C) \end{cases} \tag{10}$$

Taking into account the formulas (10), the derivatives of the acceleration energy:

$$\frac{\partial S}{\partial \ddot{\pi}_1} = m\ddot{x}_{1C}\frac{\partial \ddot{x}_{1C}}{\partial \ddot{\pi}_1} + m\ddot{y}_{1C}\frac{\partial \ddot{y}_{1C}}{\partial \ddot{\pi}_1} + m\ddot{z}_{1C}\frac{\partial \ddot{z}_{1C}}{\partial \ddot{\pi}_1} + I\ddot{\pi}_1 =$$

$$= I\ddot{\pi}_1 - \lambda m\left[(R - z_C)\left(\ddot{y}_{1O} + \ddot{y}_C\right) + y_C \ddot{z}_C\right]$$

$$\frac{\partial S}{\partial \ddot{\pi}_2} = m\ddot{x}_{1C}\frac{\partial \ddot{x}_{1C}}{\partial \ddot{\pi}_2} + m\ddot{y}_{1C}\frac{\partial \ddot{y}_{1C}}{\partial \ddot{\pi}_2} + m\ddot{z}_{1C}\frac{\partial \ddot{z}_{1C}}{\partial \ddot{\pi}_2} + I\ddot{\pi}_2 =$$

$$= I\ddot{\pi}_2 + \lambda m\left[(R - z_C)\left(\ddot{x}_{1O} + \ddot{x}_C\right) + x_C \ddot{z}_C\right]$$

$$\frac{\partial S}{\partial \ddot{\pi}_3} = m\ddot{x}_{1C}\frac{\partial \ddot{x}_{1C}}{\partial \ddot{\pi}_3} + m\ddot{y}_{1C}\frac{\partial \ddot{y}_{1C}}{\partial \ddot{\pi}_3} + m\ddot{z}_{1C}\frac{\partial \ddot{z}_{1C}}{\partial \ddot{\pi}_3} + I\ddot{\pi}_3 =$$
$$= I\ddot{\pi}_3 + \lambda m\left[y_C(\ddot{x}_{1O}+\ddot{x}_C) - x_C(\ddot{y}_{1O}+\ddot{y}_C)\right]$$

Now the Gibbs-Appell equations (8) take the following form [11]:

$$\begin{cases} I\ddot{\pi}_1 - \lambda m\left[(R-z_C)(\ddot{y}_{1O}+\ddot{y}_C) + y_C\ddot{z}_C\right] = mg\lambda y_C \\ I\ddot{\pi}_2 + \lambda m\left[(R-z_C)(\ddot{x}_{1O}+\ddot{x}_C) + x_C\ddot{z}_C\right] = -mg\lambda x_C \\ I\ddot{\pi}_3 + \lambda m\left[y_C(\ddot{x}_{1O}+\ddot{x}_C) - x_C(\ddot{y}_{1O}+\ddot{y}_C)\right] = 0 \end{cases}$$

or taking into account the notation in (7)

$$\begin{cases} \dot{\omega}_x = \alpha\left[(R-z_C)(\ddot{y}_{1O}+\ddot{y}_C) + y_C(\ddot{z}_C+g)\right] \\ \dot{\omega}_y = -\alpha\left[(R-z_C)(\ddot{x}_{1O}+\ddot{x}_C) + x_C(\ddot{z}_C+g)\right] \\ \dot{\omega}_z = -\alpha\left[y_C(\ddot{x}_{1O}+\ddot{x}_C) - x_C(\ddot{y}_{1O}+\ddot{y}_C)\right] \end{cases} \quad (11)$$

де $\alpha = \frac{\lambda}{\rho^2}$, $\rho^2 = \frac{I}{m}$ – the square of the ball's radius of inertia.

For the following, it is reasonable to write the equation in the form:

$$\begin{cases} \dot{\omega}_x = \alpha_{12}\ddot{y}_C + \alpha_{13}\ddot{z}_C + \beta_1 \\ \dot{\omega}_y = \alpha_{21}\ddot{x}_C + \alpha_{23}\ddot{z}_C + \beta_2 \\ \dot{\omega}_z = \alpha_{31}\ddot{x}_C + \alpha_{32}\ddot{y}_C + \beta_3 \end{cases} \quad (12)$$

where:

$\alpha_{12} = -\alpha_{21} = \alpha(R-z_C)$, $\alpha_{13} = -\alpha_{31} = \alpha y_C$, $\alpha_{23} = -\alpha_{32} = -\alpha x_C$,

$\beta_1 = \alpha\left[(R-z_C)\ddot{y}_{1O} + y_C g\right]$, $\beta_2 = -\alpha\left[(R-z_C)\ddot{x}_{1O} + x_C g\right]$,

$\beta_3 = -\alpha(y_C\ddot{x}_{1O} - x_C\ddot{y}_{1O})$.

The differential equations (12) should be integrated together with the expressions of the nonholonomic elms (6), which are in fact also differential equations.

The right-hand sides of equations (12), (6) should be expressed in terms of x_C, y_C, ω_x, ω_y, ω_z.

To transform the Gibbs-Appell equations into Cauchy differential equations, it is not possible to integrate equations (12) and (6) directly using widely used numerical algorithms. The equations must be represented in Cauchy form, i.e. solved in terms of the derivative of one of the functions to be found. In the case at hand – $\dot{\omega}_x$, $\dot{\omega}_y$, $\dot{\omega}_z$, $\dot{x}_C$, $\dot{y}_C$. Equations (6) have the following structure. However, the right-hand sides of equation (12) also depend on $\dot{\omega}_x$, $\dot{\omega}_y$, $\dot{\omega}_z$ (see formulae (10) and (7)), so these equations must be solved in terms of these derivatives. If the matrix formed by the coefficients of the derivatives $\dot{\omega}_x$, $\dot{\omega}_y$, $\dot{\omega}_z$ the corresponding system of linear equations had constant elements, then finding the inverse of it and representing the equations in a form suitable for numerical integration would be a trivial task. Since the elements of the matrix are variable, finding its inverse is a time-consuming operation. In the numerical implementation of the algorithm, it proved preferable to solve the system of equations (12) with respect to $\dot{\omega}_x$, $\dot{\omega}_y$, $\dot{\omega}_z$ using Kramer's formulae. Finally, the system of differential equations (12) and (6) in the Cauchy form takes the following form:

$$\begin{cases} \dot{\omega}_x = f_{\omega_x}(\omega_x,\omega_y,\omega_z,x_C,y_C,t) \\ \dot{\omega}_y = f_{\omega_y}(\omega_x,\omega_y,\omega_z,x_C,y_C,t) \\ \dot{\omega}_z = f_{\omega_z}(\omega_x,\omega_y,\omega_z,x_C,y_C,t) \\ \dot{x}_C = f_{x_C}(\omega_x,\omega_y,\omega_z,x_C,y_C,t) \\ \dot{y}_C = f_{y_C}(\omega_x,\omega_y,\omega_z,x_C,y_C,t) \end{cases} \quad (13)$$

where

$$f_{\omega_x}(\omega_x,\omega_y,\omega_z,x_C,y_C,t) = \frac{\Delta_1(\omega_x,\omega_y,\omega_z,x_C,y_C,t)}{\Delta(x_C,y_C)},$$

$$f_{\omega_y}(\omega_x,\omega_y,\omega_z,x_C,y_C,t) = \frac{\Delta_2(\omega_x,\omega_y,\omega_z,x_C,y_C,t)}{\Delta(x_C,y_C)},$$

$$f_{\omega_z}(\omega_x,\omega_y,\omega_z,x_C,y_C,t) = \frac{\Delta_3(\omega_x,\omega_y,\omega_z,x_C,y_C,t)}{\Delta(x_C,y_C)},$$

$$\Delta(x_C,y_C) = a_{11}a_{22}a_{33} + a_{12}a_{23}a_{31} + a_{21}a_{32}a_{13} - a_{31}a_{22}a_{13} - a_{21}a_{12}a_{33} - a_{32}a_{23}a_{11},$$

$$\Delta_1(x_C,y_C) = b_1a_{22}a_{33} + a_{12}a_{23}b_3 + b_2a_{32}a_{13} - b_3a_{22}a_{13} - b_2a_{12}a_{33} - a_{32}a_{23}b_1,$$

$$\Delta_2(x_C,y_C) = a_{11}b_2a_{33} + b_1a_{23}a_{31} + a_{21}b_3a_{12} - a_{31}b_2a_{13} - a_{21}b_1a_{33} - b_3a_{23}a_{11},$$

$$\Delta_3(x_C,y_C) = a_{11}a_{22}b_3 + a_{12}b_2a_{31} + a_{21}a_{32}b_1 - a_{31}a_{22}b_1 - a_{21}a_{12}b_3 - a_{32}b_2a_{11},$$

$$f_{x_C}(\omega_x,\omega_y,\omega_z,x_C,y_C,t) = \lambda\left[\omega_y(R-z_C) + \omega_z y_C\right],$$

$$f_{y_C}(\omega_x,\omega_y,\omega_z,x_C,y_C,t) = -\lambda\left[\omega_x(R-z_C) + \omega_z x_C\right],$$

$\delta_1 = \lambda(\omega_z\dot{y}_C - \omega_y\dot{z}_C)$, $\delta_2 = \lambda(\omega_x\dot{z}_C - \omega_z\dot{x}_C)$,

$$\delta_3 = \frac{\lambda}{R-z_C}\left[(\omega_z y_C - \omega_y x_C)\dot{z}_C + \omega_z(x_C\dot{y}_C - y_C\dot{x}_C)\right] + \frac{\dot{x}_C^2 + \dot{y}_C^2 + \dot{z}_C^2}{R-z_C},$$

$a_{11} = 1 + \rho^2(\alpha_{12}^2 + \alpha_{13}^2)$, $a_{12} = a_{21} = \rho^2\alpha_{13}\alpha_{23}$,

$a_{13} = a_{31} = -\rho^2\alpha_{12}\alpha_{23}$, $a_{22} = 1 + \rho^2(\alpha_{12}^2 + \alpha_{23}^2)$,

$\alpha_{23} = \alpha_{32} = \rho^2\alpha_{12}\alpha_{13}$, $a_{33} = 1 + \rho^2(\alpha_{13}^2 + \alpha_{23}^2)$,

$b_1 = \alpha_{12}\delta_2 + \alpha_{13}\delta_3 + \beta_1$, $b_2 = -\alpha_{12}\delta_1 + \alpha_{23}\delta_3 + \beta_2$,

$b_3 = -\alpha_{13}\delta_1 - \alpha_{23}\delta_2 + \beta_3$.

The initial conditions for the Cauchy problem in this form are as follows [21]:

at $t = 0$, $\omega_x = \omega_{x0}$, $\omega_y = \omega_{y0}$, $\omega_z = \omega_{z0}$, $x_C = x_{C0}$, $y_C = y_{C0}$

In this case, the law of motion of the spherical camera should be given by:

$$x_{1O} = x_{1O}(t),\ y_{1O} = y_{1O}(t) \quad (14)$$

Thus, the mathematical model of the device, after schematisation, is a system with nonholonomic couplings. This circumstance greatly complicates the solution of the problem, which is one of the reasons why such problems are relatively rarely considered in the dynamics of machines and mechanisms. In particular, after the mathematical model of the dynamic processes in a ball mill was presented in the form of the Gibbs-Appell equations, their transformation into the Cauchy equations taking into account nonholonomic viscosities (for further numerical integration) was practically possible only with the use of symbolic mathematics implemented in modern mathematical packages, due to their complexity and tediousness. For further calculations, the symbolic processor of the MathCAD mathematical package was used to create the corresponding computer programs [10].

After integrating the differential equations of motion (13), it is possible to determine two important technological characteristics of the device: the trajectory of the point of contact of the ball on the internal surface of the spherical chamber; the force of pressure of the ball on the chamber (modulo coinciding with the radial reaction of the shell).

To determine the trajectory of the point of contact between the ball and the sphere, we use the proportionality condition (see Fig. 2):

$$x_P = \frac{R}{R-r}x_C,\ y_P = \frac{R}{R-r}y_C,\ z_P = \frac{R}{R-r}(z_C - r)$$

In order to determine the force of the ball pressure force on the chamber, it is necessary to determine the radial reaction of the ball, using the well-known theorem on the movement of the center of mass [6]:

$$m\mathbf{a}_C = \mathbf{R}^{(e)} \quad (15)$$

where $\mathbf{a}_C = a_{Cx_1}\mathbf{i}_1 + a_{Cy_1}\mathbf{j}_1 + a_{Cz_1}\mathbf{k}_1 = a_{Cx}\mathbf{i} + a_{Cy}\mathbf{j} + a_{Cz}\mathbf{k}$ – center

of mass acceleration ($\boldsymbol{i}_1$, $\boldsymbol{j}_1$, $\boldsymbol{k}_1$ – unit vectors of the coordinate system axes $O_1x_1y_1z_1$; $\boldsymbol{i}$, $\boldsymbol{j}$, $\boldsymbol{k}$ – unit vectors of the coordinate system axes $Oxyz$); $\boldsymbol{R}^{(e)}$ – the main vector of external forces applied to the ball.

In this case, expression (15) takes the form:

$$m\mathbf{a}_C = m\mathbf{g} + \mathbf{N} + \mathbf{F}_{fr} \tag{16}$$

where $m\boldsymbol{g}$ – gravity (see Fig. 2); $\boldsymbol{N}$ – radial (normal) reaction; $\boldsymbol{F}_{fr}$ – friction force located in the tangential plane (not shown in Fig. 2).

It should be noted that expression (16) is one of the equations of the kinetostatics method (Dalembert's principle). Let us denote the acute angles formed by the vectors $\boldsymbol{i}$, $\boldsymbol{j}$, $\boldsymbol{k}$ with the line CA by α, β, γ, respectively [14].

The following expressions are valid for the cosines of these angles (see Fig. 2):

$$\cos\alpha = \frac{x_C}{R-r},\ \cos\beta = \frac{y_C}{R-r},\ \cos\gamma = \frac{R-z_C}{R-r} \tag{17}$$

Now let's project expression (16) onto the $C\zeta$ axis, directed from point C to point A (see Fig. 2):

$$-ma_{Cx_1}\cos\alpha - ma_{Cy_1}\cos\beta + ma_{Cz_1}\cos\gamma = -mg\cos\gamma + N_\zeta + F_{fr_\zeta}$$

Since the friction force is perpendicular to the normal, $F_{fr\zeta} = 0$ and from the last expression for the normal reaction we have $N = N_\zeta = -m(a_{Cx_1}\cos\alpha + a_{Cy_1}\cos\beta - (a_{Cz_1} + g)\cos\gamma)$ or finally taking into account formulas (17):

$$N = -m\left(a_{Cx_1}\frac{x_C}{R-r} + a_{Cy_1}\frac{y_C}{R-r} + (a_{Cz_1} + g)\frac{z_C - R}{R-r}\right) \tag{18}$$

Acceleration projections based on formulas (10):

$$a_{Cx_1} = \ddot{x}_{1C} = \ddot{x}_{1O} + \ddot{x}_C,\ a_{Cy_1} = \ddot{y}_{1C} = \ddot{y}_{1O} + \ddot{y}_C,\ a_{Cy_1} = \ddot{z}_{1C} = \ddot{z}_C$$

However, as a result of the numerical integration of the differential equations (13), only the values of x_C, y_C, z_C at discrete points in time are determined ($x_{1O}(t)$, $y_{1O}(t)$ are known functions). In this situation, symbolic mathematics also allows to effectively determine the values of the second derivatives $\ddot{x}_C$, $\ddot{y}_C$, $\ddot{z}_C$ in this situation. In the programs developed, the functions $\ddot{x}_C$, $\ddot{y}_C$, $\ddot{z}_C$ are first constructed using the cubic spline approximation with discrete values of t and x_C, y_C, z_C. Then, using a symbolic processor, analytical expressions for $\ddot{x}_C(t)$, $\ddot{y}_C(t)$, $\ddot{z}_C(t)$ are found [13].

To simulate the starting of a device with an electric motor, it is necessary to formulate the law of motion of a spherical chamber (14). In this case, it is assumed that the dependence of the angular velocity of the rotor of the electric motor on the time when the device is switched on has the form shown in the graph in Figure 3 [1, 10].

For the time interval $0 \le t = t_0$, the quadratic law of the angular velocity change was taken, which is in good agreement with the experimental data. The time dependence of the rotation angle of the motor rotor in this case is as follows:

$$\psi = \begin{cases} -\dfrac{\omega_0(t-t_0)^3}{3t_0^2} + \omega_0 t - \dfrac{\omega_0 t_0}{3}, & t \le t_0 \\ \dfrac{2}{3}\omega_0 t_0 + \omega_0(t-t_0), & t > t_0 \end{cases}$$

where ω_0 – steady-state angular velocity of the mode (controllable parameter); t_0 – installation time.

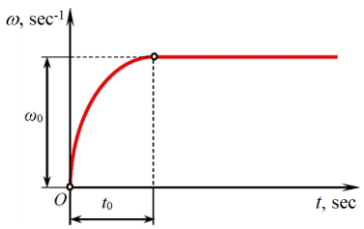

Fig. 3. The law of angular velocity change of an electric motor during start-up

3. Results and discussion

The developed mathematical model of the dynamic processes in a ball mill is the basis of the algorithm implemented using the MathCAD software package. To solve the differential equations, the fourth-order Runge–Kutta method was used (the Rkadapt function in MathCAD was applied, which employs a variable step size in its internal computations and returns an approximate solution on a uniform grid). The studies using the developed programme were carried out for the following values of the mill parameters: r = 0.025 m – ball radius; R = 0.25 m – radius of the spherical chamber; l = 0.5 m – length of the crank; n_0 = 60.0 min^{-1} – steady-state crank rotation frequency [9].

Figure 4 shows the dependence of the application z_P on the contact point between the ball and the chamber P during the "fast" start of the apparatus; the set-up time is t_0 = 2.5 sec.

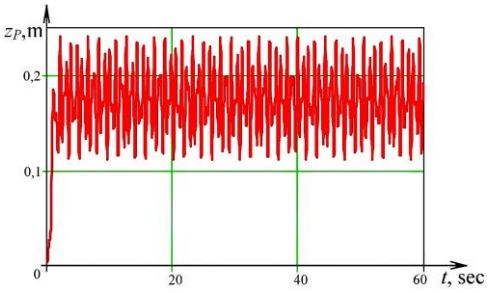

Fig. 4. Dependence of the coordinate z_P of the point of contact on time (t_0 = 2.5 sec)

The corresponding trajectory in the Oxy plane is shown in Fig. 5. In fact, it is a kind of «ring» of considerable width.

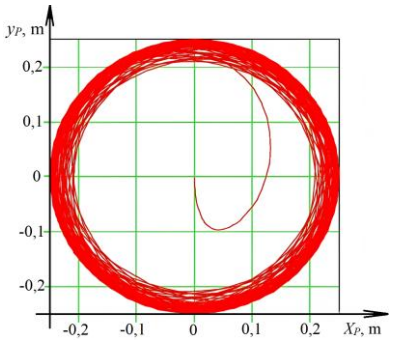

Fig. 5. Trajectory of the point of contact between the ball and the sphere in the projection on the Oxy plane (t_0 = 2.5 sec)

These graphs show that there is no tendency for the ball to reach a particular steady state in its motion. This is because the dynamic model of the first stage mill does not take energy dissipation into account. The trajectory forms a ring of greater width the shorter the launch. This is illustrated by the graphs in Figures 6 and 7. In contrast to the graphs in Figures 4 and 5, these are plotted for a 'slow' launch; the settling time is t_0 = 30.0 sec.

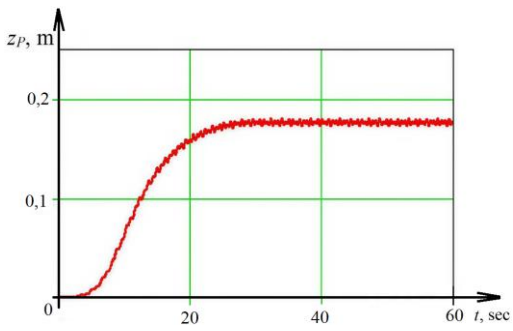

Fig. 6. Dependence of the z_P coordinate of the touch point on time (t_0 = 30.0 sec)

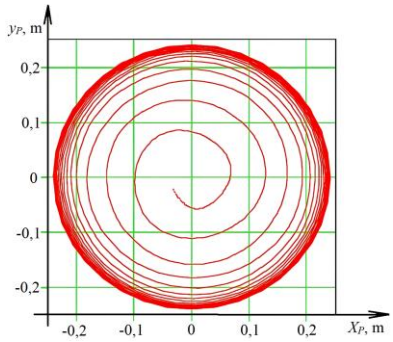

Fig. 7. Trajectory of the point of contact between the ball and the sphere in the projection on the Oxy plane (t_0 = 30.0 sec)

The graphs in Figures 8 and 9 illustrate the nature of the change in pressure of the ball on the cup during the "fast" and "slow" start-up of the apparatus. For a set-up time of t_0 = 2.5 sec, the pressure variations reach 9.0 N; for a long start-up (t_0 = 30.0 sec) they are less than 1.0 N.

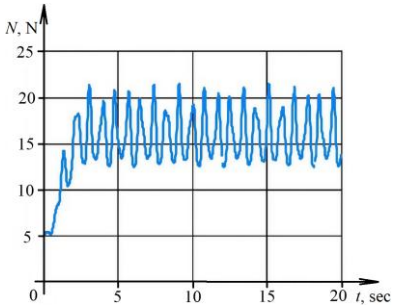

Fig. 8. Dependence of the ball pressure force on the chamber on time (t_0 = 2.5 sec)

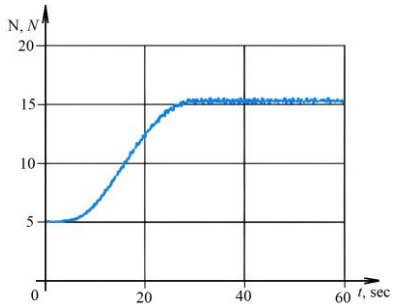

Fig. 9. Dependence of the ball pressure force on the chamber on time (t_0 = 30.0 sec)

4. Conclusions

1. The specific features of technical systems in which the main functional component is a ball moving within a spherical cavity have been analyzed.
2. A mathematical model of the dynamic processes occurring in a ball mill has been developed and represented as a system of differential equations describing the motion of a ball inside a spherical shell performing a circular translational motion.
3. The equations of motion have been formulated in the framework of Gibbs-Appell equations, where the introduction of quasi-velocities proved to be an efficient approach for expressing acceleration functions.
4. An algorithm has been proposed for transforming Gibbs-Appell equations into a system of first-order differential equations in the Cauchy form.
5. A method has been proposed to represent the time-dependent behavior of the angular velocity of the drive electric motor during the start-up phase of the device.
6. An algorithm has been proposed for constructing the trajectories of the contact point of the ball with the inner surface of the spherical chamber.
7. An algorithm has been developed for determining the pressure force acting on the spherical shell of the ball during its motion.
9. It has been shown that the “ring” formed by the trajectories of the ball’s contact point with the spherical shell becomes wider as the start-up process of the device becomes faster.
10. It has been established that the amplitude of pressure oscillations exerted by the ball on the spherical shell during rapid start-up can significantly exceed the corresponding amplitudes observed during slow start-up.
11. The most important direction for further improvement of the dynamic model of the ball mill is a more accurate description of the interaction between the ball and the shell, taking into account the resistance of the processed mixture to the ball’s rolling motion.
12. The next stage of research involves the development of a comprehensive dynamic model of the device that incorporates the dynamic characteristics of the drive motor. During start-up and steady-state operation, the motor is subjected to oscillatory loads, resulting in mutual influence between the dynamic processes in the motor (due to its limited power) and in the ball mill itself. Since the asynchronous electric motor is the simplest, most cost-effective, and operationally convenient option, it becomes essential to accurately describe its dynamic characteristics and integrate them into the overall model. The creation of an energy-efficient device is impossible without the rational selection of the electric motor.

References

[1] Carvalho R. M. et al.: Mechanistic modeling and simulation of grinding iron ore pellet feed in pilot and industrial-scale ball mills. Powder Technology 392, 2021, 489–502 [https://doi.org/10.1016/j.powtec.2021.07.030].
[2] Dvirna O. et al.: Dynamic Processes Modeling in a Peristaltic Pump with a Hydraulic Drive for the Bingham Fluid. Advances in Science and Technology Research Journal 16(4), 2022, 256–269 [https://doi.org/10.12913/22998624/152944].
[3] Hacksteiner M., Peherstorfe H., Bleicher F.: Energy efficiency of state-of-the-art grinding processes. Procedia Manufacturing 21, 2018, 717–724 [https://doi.org/10.1016/j.promfg.2018.02.176].
[4] Hanumanthappa H. et al.: comparative study on a newly designed ball mill and the conventional ball mill performance with respect to the particle size distribution and recirculating load at the discharge end. Minerals Engineering 145(1), 2020, 106091 [https://doi.org/10.1016/j.mineng.2019.106091].
[5] Iskovych-Lototsky R. D., Ivanchuk Y. V., Veselovsky Y. P.: Simulation of Working Processes in the Pyrolysis Plant for Waste Recycling. Eastern-European Journal of Enterprise Technologies 1(8(79)), 2016, 11–20 [https://doi.org/10.15587/1729-4061.2016.59419].
[6] Le Roux J. D. et al.: Steady-state and dynamic simulation of a grinding mill using grind curves. Minerals Engineering 152, 2020, 1–21 [https://doi.org/10.1016/j.mineng.2020.106208].
[7] Legeza V.: Determination of the amplitude-frequency characteristic of the new roller damper for forced oscillations. Journal of Automation and Information Sciences 34, 2012, 32–39 [https://doi.org/10.1615/JAutomatInfScien.v34.i5.40].
[8] Legeza V. P.: Dynamics of Vibration Isolation System with a Ball Vibration Absorber. Int Appl Mech 54, 2016, 584–593 [https://doi.org/10.1007/s10778-018-0912-0].
[9] Donald T.: Greenwood, Advanced Dynamics. Cambridge University Press, Cambridge 2003 [https://doi.org/10.1017/CBO9780511800207].
[10] Manzhilevskyy O. D.: Analysis of hydraulic vibration drive machine for vibration abrasive processing. Przegląd Elektrotechniczny 1(4), 2019, 95–99 [https://doi.org/10.15199/48.2019.04.16].
[11] Náprstek J. et al.: Non-linear dynamic behaviour of a ball vibration absorber. Papadrakakis M., Fragiadakis M., Plevris V. (eds.): Computational Methods in Earthquake Engineering. Computational Methods in Applied Sciences 30. Springer, Dordrecht 2013 [https://doi.org/10.1007/978-94-007-6573-3_18].
[12] Náprstek J., Fischer C.: Dynamic behavior and stability of a ball rolling inside a spherical surface under external excitation. Zingoni A. (ed.): Insights and innovations in structural engineering, mechanics and computation. Taylor & Francis, London 2016, 214–219.
[13] Náprstek J., Fischer C.: Non-holonomic dynamics of a ball moving inside a spherical cavity. Procedia Engineering 199, 2017, 613–618 [https://doi.org/10.1016/j.proeng. 2017.09.105].
[14] Pirner M., Fischer O.: The development of a ball vibration absorber for the use on towers. Journal of the International Association for Shell and Spatial Structures 41, 2012, 91–99 [https://doi.org/10.1007/978-981-15-8049-9_1].

[15] Rizzo A., Peterson G.: Progress toward sustainable polymer technologies with ball-mill grinding. Progress in Polymer Science 159, 2024, 101900 [https://doi.org/10.1016/j.progpolymsci.2024.101900].
[16] Sabah E., Özdemir O., Koltka O.: Effect of ball mill grinding parameters of hydrated lime fine grinding on consumed energy. Advanced Powder Technology 24(3), 2013, 647–652 [https://doi.org/10.1016/j.apt.2012.12.001].
[17] Veselovska N. R. et al.: Simulation modeling of the adaptive system for hydraulic drives of a stalk forage separator. Journal of Engineering Sciences 12(1), 2025, F8–F17 [https://doi.org/10.21272/jes.2025.12(1).f2].
[18] Viguié R., Kerschen G.: Nonlinear vibration absorber coupled to a nonlinear primary system: A tuning methodology. Journal of Sound and Vibration 326(3-5), 2019, 780–793 [https://doi.org/10.1016/j.jsv.2009.05.023].
[19] Wang T.: Assessing load in ball mill using instrumented grinding media. Minerals Engineering 173(1), 2021, 107198 [https://doi.org/10.1016/j.mineng.2021.107198].
[20] Zhang X. et al.: Effect of different mills on the fine grinding characteristics and leaching behaviour of gold ore. Minerals Engineering 2024, 215108800 [https://doi.org/10.1016/j.mineng.2024.108800].
[21] Zhengbing H. et al.: Mathematical Model of the Damping Process in a One System with a Ball Vibration Absorber. Int. J. Intelligent Systems and Applications (IJISA) 10(1), 2018, 24–33 [https://doi.org/10.5815/ijisa.2018.01.04].

Prof. Volodymyr M. Shatokhin
e-mail: shatokhinvlm@gmail.com

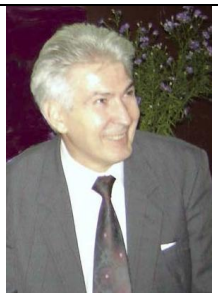

He is Doctor of Technical Sciences, professor of the Department of Theoretical and Applied Mechanics, O. M. Beketov National University of Urban Economy in Kharkiv (Ukraine). Author of 200 scientific and methodological publications.
Research interests: machine dynamics, nonlinear oscillations, nonlinear integral equations, dynamic processes in hydraulic transmissions, dynamic processes in mechanical systems with electric drive, synthesis of machines and mechanisms.

https://orcid.org/0000-0002-0766-4104

Prof. Yaroslav V. Ivanchuk
e-mail: ivanchuck@ukr.net

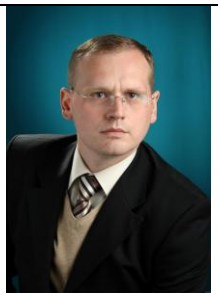

He is Doctor of Technical Sciences, professor of the Department of Computer Science, Vinnytsia National Technical University (Ukraine). Scientific Secretary of the Specialized Scientific Council with the award of the academic degree of Doctor of Science. Member of the editorial board of international scientific and technical journals. Interests: mathematical modeling of complex systems and computational methods.

https://orcid.org/0000-0002-4775-6505

Ph.D. Vitaly V. Liman
e-mail: limanv@ukr.net

He is Ph.D. in technique, associate professor of the Department of Computer Science and Economic Cybernetics, Vinnytsia National Agrarian University (Ukraine). Author of 60 scientific publications, including 45 scientific articles in professional journals, 15 patents for inventions.
Researche interests: Web technologies, internet marketing.

https://orcid.org/0000-0003-1280-237X

Ph.D. Sergii V. Komar
e-mail: sergey.komar.kh@gmail.com

He is Ph.D. in technique, associate professor of the Department of Aeronautical Engineering, Ivan Kozhedub Kharkiv National University of the Air Force (Ukraine). Author of 80 scientific publications, including 60 scientific articles in professional journals, 12 patents for inventions. Researche interests: theory of automatic control and issues of aircraft control systems and aircraft power plants.

https://orcid.org/0000-0002-8961-2614

M.Sc. Oleksii A. Kozlovskyi
e-mail: ak@vin.ua

Master's degree of Vinnytsia National Technical University (Ukraine).
Research interests: methods and systems of artificial intelligence, computer modeling of technological processes.

https://orcid.org/0009-0008-1797-4086